TEST Engineering & Management

January-February 2020
ISSN: 0193-4120 Page No. 15024 - 15029

On the FIB Fabrication of Nano-Gap Metal Electrodes and Nature of their I-V Characteristics

[1]Abhishek Kumar Singh, [2]Amit Kumar, [3]Saket Kumar
[1] Department of Physics, Darbhanga College of Engineering, Darbhanga, Bihar,
[3]Department of ECE
Department of EEE, Darbhanga College of Engineering, Darbhanga, Bihar, India-846005
Institute of Technology, Muzaffarpur, Bihar, India
[1]abhis.iitk@gmail.com, [2]amit.kumarc210@gmail.com, [3]sgsaket1@gmail.com

Article Info
Volume 82
Page Number: 15024 - 15029
Publication Issue:
January-February 2020

Article History
***Article Received**: 18 May 2019*
***Revised**: 14 July 2019*
***Accepted**: 22 December 2019*
***Publication**: 28 February 2020*

Abstract:
Copper and platinum electrodes with a nano-gap of ~100 nm have been fabricated by milling of thin metallic films by a focused ion beam (FIB) system. The current-voltage (I-V) characteristics of platinum electrodes are shown to follow V3/2 dependence in accordance with the classical Child-Langmuir's law while those of copper electrodes measured inside the FIB chamber (residual pressure of ~10-6mbar) correspond to tunneling at low voltage and Fowler-Nordheim (F-N) quantum mechanical tunneling above 8.4V. The field enhancement factor (β) is found to depends on the surface homogeneity, cross-sectional area, gap of electrodes, and varies inversely with the applied voltage (value lies in the range of 8-21).

Keywords: *Focused ion beam, Nanostructure fabrication, SEM.*

I. INTRODUCTION

The fabrication and electrical transport properties of nano-gap electrodes have become important in emerging electronics today because of their wide-ranging applications in high brightness /low power flat-panel displays, sensors, e-beam lithography (EBL), high power microwave amplifiers, sub-100nm transistor circuits, field emission electron sources, etc. [1-5]. Also, they make reliable electrical contacts at the nanoscale, bridge individual nano-structure with the macroscopic system, and realize devices for detecting nano-particles [6-8]. The nanogap electrodes are formed by electron beam lithography (EBL) [9], shadow evaporation [10], mechanically controllable break junction (MCB) [11], electrochemical plating [12] and electromigration [3, 13]. Yet, another technique based on focused ion beam (FIB)-direct lithography has attracted increasing interest in the recent past [14]. This enables direct mask-less fabrication of nanogap electrodes by sputter milling of the metal thin film with a fine (<10 nm) ion beam besides a variety of three-dimensional structure of nanostructures, namely pillars, cantilevers, springs, etc. (needed for various nano/micro-electromechanicalsystems), nanosensors, actuators, and structures for biological applications [15]. The technique is quick and flexible, suited for nanostructure fabrication [16]. The FIB has provided a very convenient tool for building features through a combination of gradual addition and removal of material [17]. This paper describes the fabrication of i) planar metallic nanoelectrode over the substrate by milling the metallic film and ii) case of overhanging nanoelectrode by involving a judicious combination of milling and deposition of metallic films with FIB. Further, their I-V characteristics have been studied under the ambient condition as well as inside the FIB chamber, maintained at a residual pressure of 10^{-6} mbar.

II. EXPERIMENTAL DETAILS

Focused ion beam (FIB) model FEI Nova Nanolab 600 equipped with energy-dispersive X-ray spectroscopy (EDS) facilities for compositional

January-February 2020
ISSN: 0193-4120 Page No. 15024 - 15029

analyzing of the samples and Residual Gas Analyzer (RGA) for identifying the gases present in the vacuum chamber. The I-patterned mask has been used for Cu deposition on which the electrical connections have been made. The 30 KeV ion energy with current ranging from 10 pA to 0.1 nA and dwell time varying from 100 ns to 1 ms have A thin film of I-shape and thickness ~150-200 nm is initially deposited by d.c. sputtering on a cleaned glass substrate with a d.c. sputtering unit (fig. 1). A trench is then created by milling the platinum film of length 200μm and width 100 nm using a dual-beam focused ion beam (FIB) with 30keV Ga^+ ions beam size ~10-20 nm at current ~100 pA [18].

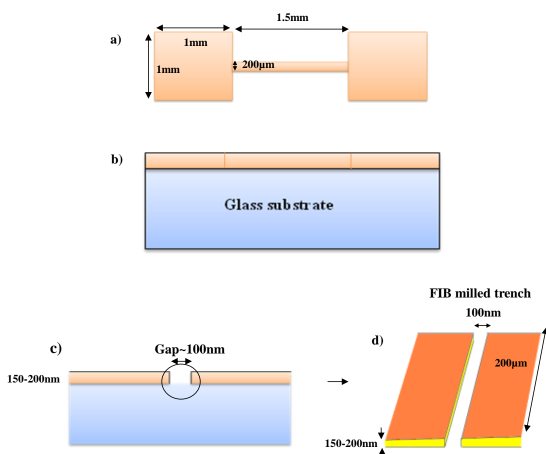

Figure 1:Schematic diagram of a) an I-shape pattern of metal film deposited on glass substrate by using thermal evaporation b, c) cross-sectional view before and after forming a trench (width ~ 100 nm) by milling with the focused ion beam, and d) nanoelectrodes of size 200 μm x 150-200 nm with a gap of ~ 100 nm.

Thus, the electrodes of a cross-sectional area 200μm x 150-200nm and a gap of 100nm are realized. The cross-section view of the platinum film with between the gap electrodes and schematic picture of 100 nm wide trench created are shown in Fig. 2.The electrodes assembly with the gap has been placed on a specially designed sample holder for measuring current-voltage (I-V) characteristics in air and/or vacuum by employing a current source, Keithley model 6430.

III. Results And Discussions

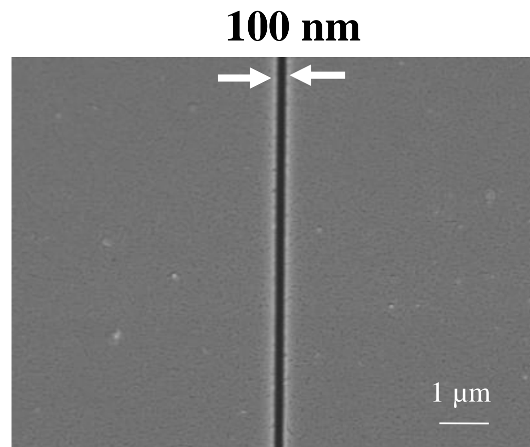

Figure 2: Scanning electron micrograph of electrodes with a gap of 100nm.

The current density (J) versus voltage (V) plot on a log scale (inset of fig. 4) shows a straight line with a slope of ~1.5 in the voltage range of ~11-35V, suggesting thereby the operation of the classical Child-Langmuir's law, i.e., $V^{3/2}$ dependence [19, 20].

$$J_{CL} = \frac{4\varepsilon_0}{9}\sqrt{\frac{2e}{m}}\frac{V^{3/2}}{D^2} \qquad \text{............(1)}$$

where ε_0 is the permittivity of free space, e is the charge of an electron, D is the gap between the electrode strips of cross-section (infinite length and width W; D/W<0.1) and m is mass of an electron. Nevertheless, the actual current value is quite different, i.e., seven order smaller than predicted by the empirical Child-Langmuir law in 2-dimension for D=100 nm [20]. On the other hand, the observed values do match with quantum space charge limited current (J_{QM}) without showing the expected $V^{1/2}$ dependence [21],

$$J_{QM} = \frac{\varepsilon_0 h^2}{4\pi^2 e^{1/2} m^{3/2}}\left[\frac{V^{1/2}}{D^4}\right]$$

..................(2)

The above assertions become apparent from fig.3 and fig.4 in which J-V plots are drawn on a log and semi-log scales using Child-Langmuir (CL) and quantum space charge (QM) formulations (eqs.1 and

January-February 2020
ISSN: 0193-4120 Page No. 15024 - 15029

2 respectively) for electrodes having a gap of 100nm. Notice that in both the cases (fig. 4, 5), $J_{CL} >> J_{QM}$ and so quantum effects are insignificant in this situation.

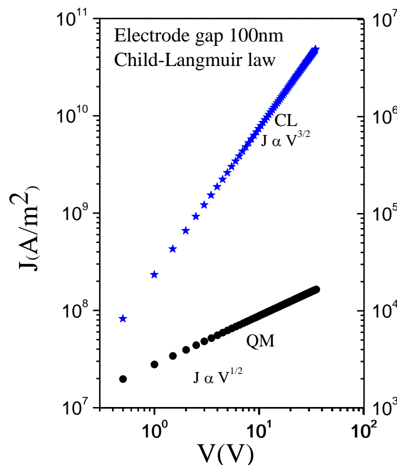

Figure 3:Current density versus voltage (J-V) characteristics on semi-log scale platinum electrodes formed with a gap of 100 nm on the glass substrate. Inset gives the (J-V) plot on a log scale with a straight line of slope ~ 1.48 above 10 V, depicting the $V^{3/2}$ dependence of current.

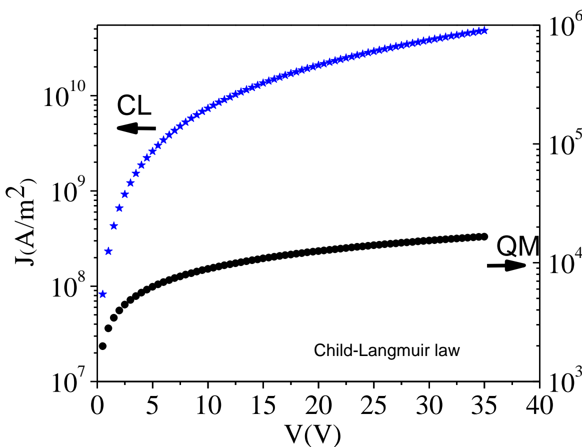

Figure 4:J-V characteristics of metal electrodes with a gap of 100nm obtained from classical Child-Langmuir (CL) law and quantum space charge limited current (QM), i.e., $V^{3/2}$ and $V^{1/2}$ dependence.

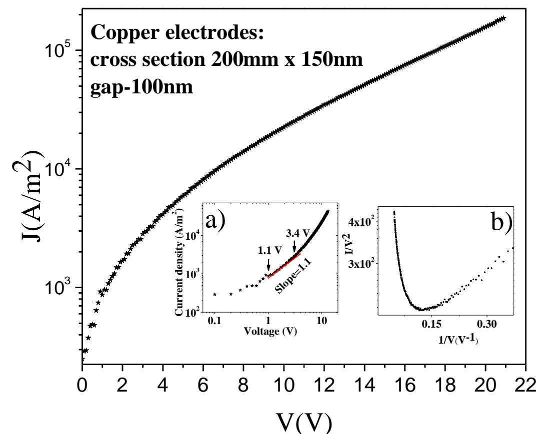

Figure 5: J-V characteristics of copper electrodes having a gap formed on a glass substrate obtained inside the FIB column at vacuum~10-6 mbar.

Inset a) shows the J-V plot on a log scale as a straight line with a slope of 1.1 and b) depicts the (I/V2) versus 1/V plot. Fig.5 depicts the current density versus voltage plot under vacuum ~10-6 mbar on a semi-log scale for copper electrodes separated by a gap of 100nm. The corresponding J versus V plot on a log scale (in the inset) shows a straight line in the intermediate voltage regime of 1.1-3.4 V with unit slope and so suggests ohmic behavior at low-voltages; resistance being~45MΩ. Such behavior may, however, be attributed to tunneling, being valid at low voltages (IαV; for V<) [22]

Also, log (I/V^2) versus 1/V plot included in the inset contains a straight line with a negative slope above 8.4V in accordance with the Fowler-Nordheim (F-N) quantum mechanical tunneling [23].

$$I = \frac{sa}{\phi}\left[\frac{\beta V}{d}\right]^2 \exp\{-b\phi^{3/2}(\frac{D}{\beta V})\}$$

………..(3)

The value of field enhancement factor (β) deduced from the slope (magnitude being b$\phi^{3/2}$D/β) is ~175. It may be mentioned that the value of β determined similarly and reported in the literature for different systems varies markedly, i.e. lie with range 1400-30000 [24]. Therefore, the present value of β (= 175) seems to be quite reasonable. However, F-N

TEST Engineering & Management

January-February 2020
ISSN: 0193-4120 Page No. 15024 - 15029

current deduced from expression (3) with β=175 does not conform to the experimental curve shown in fig.5. Notice that (F-N) currents for β=175, 30 and 20 cross the experimental data curve at different voltages. So, it is necessary to assume variation of β itself with voltage for the observed current to follow (F-N) description. To understand this aspect, experimental data is fitted into expression (3) at each voltage taking β as a variable. Such an exercise reveals β to be inversely proportional to voltage (inset of fig.7), such that

$$\beta = \frac{A}{V} + B \qquad \text{……….(4)}$$

where constants A and B are 338V and 3.9, respectively. The typical values of β are 37.7, 26.4 and 20.8 at 10, 15, and 20 V, respectively. Thus, the current density estimated with expression (3) taking an appropriate value of β at each voltage matches well with the experimental data (fig.6). The observed current matches well with deduced value by taking β is a variable. Inset shows the variation of β inversely with the applied voltage.The change in 'β' with voltage is possibly due to surface roughness and variation in the spatial separation of electrodes. According to Bonard et al.,[24] 'β' is determined by geometrical shape, length and radius of the emitter besides impurities and localized fields at protrusions. As a consequence, the current at a given voltage becomes sufficient in regions of higher 'β' to cause local heating and blunting of the electrodes.

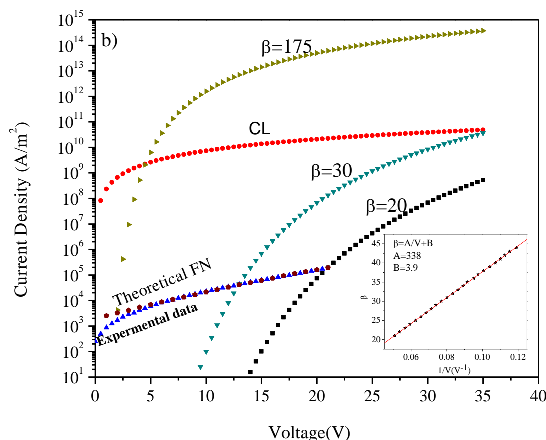

Figure 6: J-V characteristics as deduced from classical Child-Langmuir (CL) law and F-N expression with selected β values (20, 30 and 175) together with the experimental data showing the cross over.This leads to a sudden decrease in the current temporarily. On increasing voltage, the current increases again in the usual way with a new 'β' until smoothening of electrodes occurs in other regions. Fig.6 depicts this phenomenon in copper electrodes.

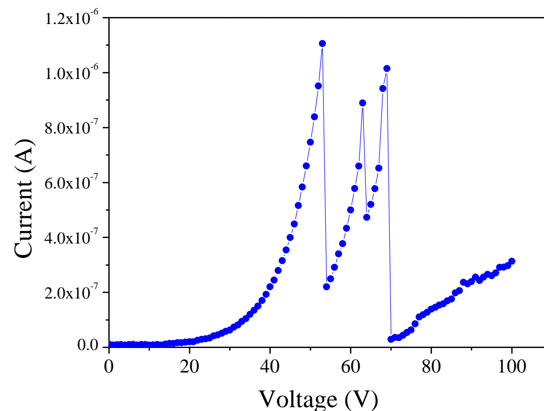

Figure 7: I-V characteristics of copper electrodes with a gap of ~ 100 nm depicting the effect of burning.

This process continues until the electrodes become smooth with nearly the same gap all over and/ or get burned out at places. Obviously, the burning process causes an overall decrease in the electrode cross-sectional area progressively.

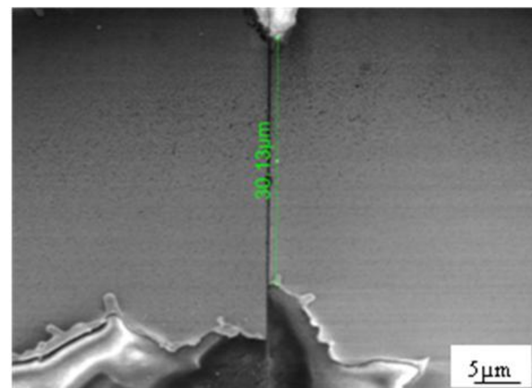

Figure 8: Scanning electron micrograph of the copper electrodes following partial burning.

The effect is displayed in the scanning electron micrograph (fig.7) with burned end regions. The J-V

TEST Engineering & Management
January-February 2020
ISSN: 0193-4120 Page No. 15024 - 15029

characteristics of the remaining portion of the electrode (30μm x 200nm, fig.9) are shown in fig.10. This result follows F-N current expression (3) above 26V now with enhancement factor (β) varying again as per exp. (4), the constants being A=294V and B=2.3. A close comparison of J-V characteristics reveals i) overall lowering of the enhancement factor (9.6 at 40 V and 8.2 at 50 V) and ii) initiation of F-N current at a higher voltage (~26V instead of 8.4V earlier fig.5). The origin of such a change lies in the electrode surface becoming relatively smooth. This result suggests that rough electrode surface and/or protrusions are responsible for large 'β' values.

CONCLUSIONS

Copper nano-gap electrodes over glass substrates and with gap ~100 nm can be fabricated successfully using a focused ion beam. copper current measurements inside the FIB chamber at a residual pressure of 10^{-6} mbar correspond to quantum tunneling at lower voltages and Fowler-Nordheim (F-N) description at voltages exceeding the metal work function. The field enhancement factor (β) varies inversely with the applied voltage, the value being in the range of 8-21.

REFERENCES

1. W. I. Milne, K. B. K. Teo, G. A. J. Amaratunga, P. Legagneux, L. Gangloff, J. P. Schnell, V. Semet, V. Thien Binhc, and O. Groeningd, "Carbon nanotubes as field emission sources," J. Mater. Chem., vol. 14, pp. 933-943, Feb. 2004.
2. K.B.K.Teo, E.Minoux, L.Hudanski, F.Peauger, J.P.Schnell, and L.Gangloff, "Microwave devices: carbon nanotubes as cold cathodes," Nature, vol. 437, pp. 968, Oct. 2005.
3. C. Durkan, M. A. Schneider, and M. E. Welland, "Analysis of failure mechanisms in electrically stressed Au nanowires," J.Appl.Phys., vol. 86, no. 03, pp. 1280-86, July 1999.
4. Q. Huang, C. M. Lilley and R. Divan, "An in situ investigation of electromigration in Cu nanowires," Nanotechnology, vol. 20, no. 07, pp. 075706, Jan. 2009.
5. P. Mandal, B. Das, and A. K. Rayachaudhuri, "Stability of a current carrying single nanowire of tungsten (W) deposited by focused ion beam," J.Appl.Phys., vol. 119, no. 08, pp. 084301-7, Feb. 2016.
6. Y. C. Lin, J. Bai, and Y. Huang, "Self-Aligned Nanolithography in a Nanogap," Nano Letters, vol. 09, no. 06, pp. 2234-2238, May 2009.
7. M. A. Reed, C. Zhou, C. J. Muller, T. P. Burgin, and J. M. Tour, "Conductance of a Molecular Junction, " Science, vol. 278, no. 5336, pp. 252-254 oct. 1997.
8. L. Malaquin, C. Vieu, M. Geneviève, Y. Tauran , F. Carcenac, M. L. Pourciel, V.Leberre, and E. Trévisiol, "Nanoelectrode-based devices for electrical biodetection in liquid solution," Microelectronic Engineering, vol. 73-74, no.01, pp. 887-892, June 2004.
9. K. Liu, Ph. Avouris, J. Bucchignano, R. Martel, S. Sun and J. Michl, "Simple fabrication scheme for sub-10 nm electrode gaps using electron-beam lithography," Appl. Phys. Lett. vol. 80, no.05, pp.865-867, Feb. 2002.
10. D. L. Klein, R. Roth, A. K. L. Lim, A. P. Alivisatos and P. L. M. Euen, "A single-electron transistor made from a cadmium selenidenanocrystal,", Nature, vol. 389, no. 699, pp. 1-3, Oct. 1997.
11. M. A. Reed, C. Zhou, C. J. Muller, T. P. Burgin and J. M. Tour, "Conductance of a Molecular Junction," Science vol. 278, 252-253, Oct. 1997.
12. A. F. Morpurgo, C. M. Marcus and D. B. Robinson, "Controlled fabrication of metallic electrodes with atomic separation," Appl.Phys.Lett., vol. 74, no. 14, 2084-2086 April 1999.
13. H. Park, A. K. L. Lim, A. Paul Alivatos, J. Park, and P. L. McEuen, "Fabrication of metallic electrodes with nanometer separation by electromigration," Appl. Phys. Lett., vol. 75, no.02, pp. 301-303, July 1999.
14. J. Melngailis, "Focused ion beam technology and applications," J.Vac.Sci.Technol.B, vol. 05, no. 02 469-494, April 1987.

TEST Engineering & Management

January-February 2020
ISSN: 0193-4120 Page No. 15024 - 15029

15. C. Satriano, S. Carnazza, A. Licciardello, S. Guglielmino, G. Marletta, "Cell adhesion and spreading on polymer surfaces micropatterned by ion beams," J. Vac. Sci. Technol. A, vol. 21 no. 04, pp. 1145-1151, Aug. 2003.
16. D. Petit, C. C. Faulkner, S. Johnstone, D. Wood, and R. P. Cowburn, "Nanometer scale patterning using focused ion beam milling," Rev.Sci. Instrum., vol. 76, pp. 026105-3, Jan. 2005.
17. S.Reyntjens and R.Puers, "A review of focused ion beam applications in microsystem technology," J. Micromech. Microeng., vol. 11, no. 04, pp. 287-300, Jan. 2001.
18. Orloff, M. Utlaut and L. Swanson, "High Resolution focused ion beams: FIB and its applications," Springer US (New York, Kluwer Academic / Plenum Publishers, 2003).
19. C. D. Child, "Discharge From Hot CaO," Phys. Rev., vol. 32, pp. 492-511, Jan. 1911.
20. J.W.Luginsland, Y.Y.Lau, and R.M.Gilgenbach, "Two-Dimensional Child-Langmuir Law," Phys. Rev. Lett. vol. 77, no. 02, pp. 4668-4670, Nov. 1996.
21. L. K. Ang, T. J. T. Kwan, and Y. Y. Lau, "New Scaling of Child-Langmuir Law in the Quantum Regime," Phys. Rev. Lett. vol. 91, no. 20, pp. 208303-4, Nov. 2003.
22. P.R.Emtage and W.Tantraporn, "Schottky Emission Through Thin Insulating Films," Phys. Rev. Lett. vol. 8, no. 07, 267-268 April 1962.
23. R.H.Fowler and L.Nordheim, "Electron Emission in Intense Electric Fields," Proc. R. Soc. Lond. A, vol. 119, no. 781, pp. 173-181, May 1928.